Original Article

# SYNERGISTIC EFFECT LUNG CANCER THERAPY: CO-DELIVERY OF QUERCETIN AND CISPLATIN VIA EUDRAGIT L-100 NANOPARTICLES *IN VITRO*

## FIRAS F. AL-MAMOORI[1,2]*, HABIBAH A. WAHAB[1], WAQAS AHMAD[1]

[1]School of Pharmaceutical Science, Universiti Sains Malaysia. [2]School of Pharmaceutical Science, University of Babylon, Iraq
*Corresponding author: Firas F. AL-Mamoori; *Email: ferasfalih2@gmail.com

## ABSTRACT

**Objective:** This study aims to investigate the potential of Eudragit L-100 nanoparticles for the co-delivery of quercetin and cisplatin to lung cancer cells, seeking to exploit the synergistic effects of the two drugs while overcoming their individual limitations.

**Methods:** We investigate the synergistic effect of co-delivering quercetin and cisplatin using Eudragit L-100 nanoparticles for lung cancer therapy. The nanoparticles were synthesized using the nanoprecipitation method, where Eudragit L-100 was dissolved in an organic solvent, followed by the incorporation of quercetin and cisplatin. The resultant nanoparticles were characterized for size, zeta potential, drug loading efficiency, and morphology using techniques such as Dynamic Light Scattering (DLS) and Scanning Electron Microscopy (SEM).

**Results:** The co-loaded Quercetin-Cisplatin Nanoparticles (Qu-Cis)-NPs formulation had a mean particle size of 475±4.77 nm. Polydispersion index of 0.266±0.093 and zeta potential was-24.03±0.89 mV. The *in vitro* cytotoxicity was assessed using normal cell and lung cancer cell lines *in vitro* studies showed that the developed nanoparticles significantly increased cancer cell mortality compared to individual drug treatments. The combination (Qu-Cis)-NPs showed more cytotoxicity on the Non-Small Lung Cancer Cell Line (NCI-H460) cancer cell line after 48 h of incubation compared to Qu loaded-NPs and Cis loaded-NPs, particularly at a concentration of 1 mg/ml. The combination showed no cytotoxicity effect on normal Human Lung fibroblast cell Lines (CCD-19 lu) cells at all concentrations after 24 h, but showed cytotoxicity effects at concentrations (0.125, 0.25, 0.5, and 1.0) mg/ml after 48 h.

**Conclusion:** The Eudragit L-100 nanoparticle system for co-delivering quercetin and cisplatin showed a promising synergistic effect in lung cancer treatment. It effectively addresses the solubility and toxicity issues of both drugs, offering a potentially more effective treatment option that merits further clinical investigation.

**Keywords:** Quercetin, Cisplatin nanoparticles, Lung cancer, Eudragit®L-100, Cytotoxic test, pH-sensitive polymer, Synergistic effect

## INTRODUCTION

Cancer remains a leading cause of death worldwide. According to the World Health Organisation, cancer is projected to become the top cause of death globally by 2025, resulting in approximately 12.7 million deaths. This staggering number accounts for nearly one in six deaths [1, 2]. The most common types of cancer include breast, lung, colon, rectum, and prostate cancer [3]. The main factors contributing to about one-third of cancer-related deaths are tobacco use, alcohol consumption, a diet lacking in fruits and vegetables, and insufficient physical activity [4]. Non-non-small lung cancer is the most common form of lung cancer, impacting both smokers and non-smokers, including individuals under the age of 45 y. In male smokers, large lung carcinoma accounts for roughly 30% of primary lung tumors, while in female smokers, it accounts for 40%. Among non-smokers, these rates are approximately 60% in males and 80% in females [5]. The most common cancer treatment approaches include chemotherapy, radiation, and surgery. These approaches can be used individually or in combination. The major challenges associated with these treatment approaches include unwanted side effects, tumor recurrence, and resistance to chemotherapy or radiation therapy [6]. The low water solubility of most chemotherapeutic agent could also pose significant therapeutic challenges. Drug candidates such as quercetin and cisplatin are poorly water-soluble, meaning that intravenous administration could cause complications like embolism and respiratory system failure due to drug precipitation, while extravascular administration could lead to poor absorption [7, 8]. Since chemotherapeutic drugs given intravenously are distributed to all tissues, including healthy ones, severe systemic side effects are possible with intravenous administration of adjuvant chemotherapy [9]. Pharmaceutical industries frequently use Eudragit® polymer, a family of commercially available acrylic acid and its derivatives, and film coating to slow the rate of drug release from tablets and capsules.

Eudragit® L-100, the most popular form of this polymer, was developed as an enteric coating. It is a Food and Drug Administration (FDA)-approved cationic polymer with a high solubility above pH 5 (pH 5.5-6.7). It is a synthetic polymer for film coating that outperforms natural products such as sugar and shellac. It has higher contents of methyl methacrylate and methacrylic acid in comparison to other Eudragit® polymers (e. g. Evonik and Eudragit® polymer). Carboxyl groups attached to the side chains of polymers are susceptible to protonation in an acidic environment, and polymers do not dissolve in acids (such as stomach acid). Nevertheless, carboxyl groups undergo ionization at neutral or basic pH [9]. It has been found that the polymer's payload is released when it becomes more soluble in water and when the negative charges between the carboxylate groups make them repel each other. The amount of carboxyl or other substituent groups on the polymer can be varied to fine-tune the pH value that governs their water solubility. The ratio of carboxyl groups to ester groups in poly-methacrylic acid-co-methyl methacrylate can be varied to modify the polymer [8]. Quercetin (Qu) is a well-known flavonoid that has been shown to have antiproliferative activity against several types of cancer, such as gastrointestinal, brain, skin and ovarian cancer, through multiple mechanisms involving free radical scavenging and chelation of transition metal ions [10]. However, quercetin has a very low water solubility (log P = 0.35) compared to the majority of other flavonoids in its category [11]. As a result of its potential activity against lung cancer, cisplatin is a chemotherapy medication used to treat various types of cancer, including lung cancer. It works by damaging the DNA of cancer cells, thereby inhibiting their ability to divide and grow. Despite its effectiveness, cisplatin has significant limitations, such as poor solubility and high toxicity, which can lead to severe side effects. This is possible due to the variation in the solubility of Eudragit® L-100 at different pH along the gastrointestinal tract (GIT). It was hypothesised that the pH sensitivity of the polymer would protect the drug as it passes

through the GIT until it reaches the lungs. Additionally, there may be a synergistic effect between quercetin and cisplatin, making the co-loaded more effective than either treatment alone in inducing growth suppression and apoptosis [11-34]. This study aimed to develop a pH-dependent Eudragit® L-100 nanocarrier to facilitate passive cellular targeting and oral delivery of anticancer drugs to lung cancer. Eudragit L-100 offers a unique combination of pH-sensitive drug release, regulatory approval, and high drug encapsulation efficiency, making it an excellent choice for co-delivery systems in lung cancer therapy.

## MATERIALS AND METHODS

### Chemicals and reagents

Quercetin was a product of Sigma-Aldrich chemicals, Cisplatin powder (cis-Diammine platinum dichloride, Mw 300.28 g/mol) Pluronic® (F-68) (average MW = ~8350 g/mol) was selected as a surface-active agent and obtained from Molekula (UK). Eudragit®L-100 (MW 13100) was a product of Evonik (Germany). Polysorbate 80 (Tw2een 80) was of Eva Chem (Ohio, USA), Potassium dihydrogen phosphate ($KH_2PO_4$) and absolute ethanol (99.5-99.8%) were supplied by J. T. Baker (Avantor Performance Materials, Phillipsburg, NJ). Ulltrapure water was produced using Milli-Q purification system (EMD Millipore, Billerica, MA, USA). Dialysis bag (analytical grade) (8.000–14.000) MWCO USA. To ensure the reproducibility of your work, here are the exact catalog numbers and manufacturers for the key reagents used in the co-delivery system of Quercetin and Cisplatin via Eudragit L-100 nanoparticles Eudragit L-100 (pH-sensitive polymer) Manufacturer: Evonik Industries, Catalog Number: 125000, Quercetin (Drug component) Manufacturer: Sigma-Aldrich Catalog Number: Q4951. Cisplatin (Drug component) Manufacturer: Sigma-Aldrich. Catalog Number: P4394Ethanol (Solvent for preparation and washing) Manufacturer: Fisher Scientific. Catalog Number: BP281850.

### Cell line and culture media

Large lung carcinoma cell line Non-Small Cell Lung Cancer Cell Line (NCI-H460), and Normal Human Lung Fibroblasts Cell Line (CCD-19Lu) were purchased from the American Type Culture Collection (ATCC), 3-[4, 5-dimethylthiazol-2-yl]2, 5-diphenyltetrazolium bromide (MTT) was purchased from HiMedia, India. Cell culture medium (RPMI-1640 Medium), Minimum Essential Medium (MEM), Fetal Bovine Serum, Penicillin-Streptomycin (antibiotic), Sodium Pyruvate, and MEM non-essential amino acids were all products of GIBCO.

### Preparation of quercetin-cisplatin nanoparticle

The solvent evaporation technique is most useful because it is simple, fast, and economical, and it also has the advantage of employing non-toxic solvents. It may be a single-emulsion method if the drug is hydrophobic and a double-emulsion method if it is hydrophilic for the preparation of co-loaded (Qu-Cis)-NPs. The single emulsion (o/w) solvent evaporation technique was followed for the preparation of Qu-loaded NPs (solvent diffusion) [35]. In brief, 50 mg of Eudragit® L-100 were dissolved in 5 ml of absolute ethanol (EtOH) according to organic volume optimization, and 0.75 mg of Qu/ml of D. W was dissolved in the Eudragit ® L-100 solution to produce a polymer/Qu solution. The cis-loaded NPs were prepared by using the double emulsion technique. Approximately 0.75 mg of cis (pure) was dissolved in each 1 ml of deionized water by heating at 35-40 °C and by ultrasonication for 2 min and stirring for 5-10 min. The concentration of 0.75 mg/ml of quercetin and cisplatin were chosen to achieve efficient drug loading and smallest particle size according to the optimisation of quercetin and cisplatin before freeze drying. This would result in a lower amount of drug being partitioned into the polymeric matrix of the NPs and a higher amount being partitioned into the external aqueous phase. The cis solution was added to a solution of Qu/Eudragit® L-100 dissolved in Ethanol (EtOH) to produce the Eudragit® L-100/Qu/Cis solution, which was mixed together for 1 min using a probe sonicator (Qsonica USA, Model Qss) at 60 % voltage efficiency at 25 °C before being added of 0.5% (w/v) of Pluronic® F-68 (w/v) to produce the final solution of co-loaded (Qu-Cis)-NPs, which was immediately stirred at 1000 rpm on a mechanical stirrer (Fisher Scientific Germany) for 3-4 h to remove the excess ethanol (EtOH).

This was followed by mixing to allow the ethanol (EtOH) to complete the evaporation of the organic solvent. The NPs were obtained by ultracentrifugation (Fisher Scientific, Germany) at 15000 rpm at 20 °C for 20 min, and the supernatant was analysed for the free drug. And the pellets were washed twice with double distilled water to remove unentrapped drugs (Qu and Cis) and adsorbed Pluronic® F-68 on the surface of the NP, and the suspension was freeze-dried for 72 h (Labcono, Model: Free Zone 4.5 l) by adding 5% (w/v) sucrose (Bendosen laboratory chemicals, MW=342.30 g/mol) as a cryoprotector [36].

### Physicochemical analysis

A portion of the formulated nanoparticles were transferred into a plastic cuvette, and the average particle size and Polydispersion Index (PDI) were determined through Dynamic Light Scattering (DLS) at 25 °C and a detection angle of 90 °C using Photon Correlation Spectroscopy (PCS). The nanoparticle dispersions were diluted in redistilled water to achieve a signal strong enough for the instrument, depending on the concentration of the drug. The zeta potential of the nanoparticles was determined using a Malvern Zetasizer (Nanoseries) (Malvern Instruments Ltd., Malvern, UK) [14].

### Determination of drug entrapment efficiency and drug content

Entrapment efficiency was estimated by the amount of unentrapped drug in the supernatant after centrifugation. Drug content was determined using High-Performance Liquid Chromatography (HPLC) with a UV detector at 370 and 210 nm according to previously described procedures [14, 15]. The drug entrapment efficiency (EE), and drug content (DC) were calculated using the formulae below.

$$EE\ (\%) = \frac{AW-EW}{TW}\ x\ 100$$

Where; AW = Actual weight of loaded drug (mg)

EW = Experimental weight of loaded drug (mg)

TW = Theoretical weight of loaded drug (mg)

$$DC\ (\%) = \frac{Weight\ of\ drug}{Total\ weight\ of\ Nanoparticles}\ x\ 100$$

### Scanning electron microscopy

A scanning electron microscope (Quta FEG 650, Hitachi S 3400, Tokyo, Japan) was used to capture images of nanoparticles in order to investigate their structure and surface morphology. To achieve this, a stub of aluminum was cut and then coated with nanoparticles using double-sided adhesive carbon tape. After air drying, gold was sputtered onto them with a sputter coater. The morphology of the coated particles were analysed using a scanning electron microscope.

### Drug-excipient interaction and polymorphism studies

Pure quercetin, Eudragit® L-100, a physical mixture of Quercetin and Eudragit® L-100, blank nanoparticles, and Qu-NP formulation were characterized using Fourier transform infrared spectrophotometry (FT-IR). About 2 mg of air-dried samples were mixed with Potassium Bromide (KBr) and compressed into discs of about 0.1 mm thick using a Mini Hand Press at a pressure of 10 tons per square meter. The IR spectra were obtained by scanning individual sample disc from 4000 to 400 cm-1 using an FT-IR spectrophotometer (Nexus FT-IR Spectrometer, Thermo Nicolet) [16].

### Powder X-ray diffractometry

The polymorphic characteristics of the blank nanoparticle, the stabiliser Pluronic® F-68, the polymer Eudragit®L-100, their physical mixture, and quercetin was determined using X-ray diffractometer (SEIFERT model JSODEBYEFLEX-2002) with the following operating conditions; temperature range-20 °C-270 °C, heating rate 5 °C/min, scanning speed 0.5°/min, scanning step 0.02/min, exposure time 3 secs, and a measuring angle range of 10-70. Each step took exactly one second, and the step size was 0.0482.

### *In vitro* cytotoxicity study (MTT-assay)

The *in vitro* cytotoxic activity of the quercetin-cisplatin nanoparticle formulations and that of free quercetin and cisplatin against Non-

Small Lung Cancer Cell Line (NCI-H460), and Normal Human Lung Fibroblasts Cell Line (CCD-19Lu) was conducted using the 3-[4, 5-dimethylthiazol-2-yl]2, 5-diphenyltetrazolium bromide (MTT) assay [19]. Type NCI-H460: It is commonly used in preclinical studies to evaluate anticancer drugs because it reflects the genetic, molecular, and pathological features of aggressive lung cancer. Researchers may select it for its ability to model the behavior of tumors and test drug efficacy, particularly for therapies targeting NSCLC. While (NCI-H460) is a well-established model, it is not the only representative NSCLC cell line. Other cell lines, such as A549 (adenocarcinoma subtype) and H1975 (harboring specific EGFR mutations), are also used depending on the specific type of NSCLC under investigation. However, NCI-H460 provides a good model for studying the more aggressive and metastatic potential of large-cell lung carcinoma. Type CCD-19Lu: Since it originates from normal lung tissue, it serves as an appropriate control to evaluate the safety and selectivity of a drug aimed at lung cancer cells.

NCI-H460 cells were cultured in RPMI-1640 (Gibco, Invitrogen, Carlsbad, CA) culture medium containing 10% Fetal Bovine Serum (FBS) (Gibco, Invitrogen, UK), 0.08 mg/ml streptomycin (Gibo, Invitrogen, UK), and incubated at 37 °C in a humidified atmosphere of 5% $CO_2$ and 95% air in sterile flasks. After a few days, when the cell density has reached $1.0 \times 10^5$ cells/$cm^2$, the cells were transferred to 96-well plates and incubated at 37 °C. When the cells became confluent, they were trypsinized and then diluted in the culture medium to achieve a total cell count of $5 \times 10^4$ cells/ml. The cell suspension was subsequently transferred to a 96-well plate at a density of 5, 000 cells per well and was left to adhere overnight. Thereafter, the cells were treated with quercetin and cisplatin nanoparticles at different concentrations (0.031, 0.063, 0.125, 0.25, 0.5, and 1.0 mg/ml) in triplicates. The treated cells were incubated at 37 °C for 24 h, and also for 48 h in two sets of experiments, after which 1 mg/ml of MTT solution was added to each well and incubated at 37 °C for 2 h in a $CO_2$ incubator. Wells containing cell-free medium were used as blank, while cells without treatment were used as the control. Finally, the culture medium was removed from each well, and 200 μl of isopropanol was added to each well to solubilise the purple formazan crystals formed. The plates were shaken, and the absorbance was read at 570 nm using an ELISA reader (Bio-Tek Instruments, Winooski, VT) at a reference wavelength of 650 nm using an Ultrospec 1100 Pro UV/Vis Spectrophotometer (Amersham Biosciences, Amersham, UK).

### Statistical analysis

Data were expressed as mean±the standard deviation (SD) of triplicates determination. Statistical analysis was performed using Microsoft Excel, version 2010. And One-way analysis of Variance (ANOVA) for comparisons involving more than two groups one-way (ANOVA) was used to determine if there were any statistically significant differences between the group means.

### RESULTS

### Physicochemical properties

The co-loaded (Qu-Cis)-NPs formulation had a mean particle size of 475±4.77 nm, which falls within the particle size range for nanoparticles. The zeta potential was-24.03±0.89 mV and the polydispersion index of 0.266±0.093. Negative zeta potential facilitates drug delivery. Nanoparticles have the advantage of being able to deliver active drugs to cancer cells by selectively using the unique pathophysiology of tumor cells, such as their enhanced permeability and retention (EPR) effect, a passive targeting mechanism that promotes tumour drug accumulation [20, 21]. The use of nanoparticles improves *in vivo* drug stability, extend active drug systemic circulation, and allow controlled drug release, resulting in an increase in drug concentration at the tumour site [22]. As shown in table 1.

**Table 1: Summarized main physicochemical properties**

| Parameters | Physicochemical properties |
|---|---|
| mean Particle size (nm) | 475±4.77 |
| Drug Entrapment Efficacy of quercetin (EE %) | 62.01±1.22 |
| Drug content concentration of quercetin (mg/ml) | 430.06±3.412 |
| Drug Entrapment Efficacy of cisplatin (EE %) | 56.62±2.43 |
| Drug content concentration of cisplatin (mg/ml) | 389.47±13.88 |
| Polydispersity index (PDI) | 0.266±0.093 |
| Zeta Potential (ZP) (Mv) | -24.03±0.89 |

Data expressed as mean±SD, n=3

### Drug entrapment efficiency and drug content

Quercetin and cisplatin entrapment in nanoparticles was calculated indirectly, and it was found that at 0.75 mg/ml, cisplatin encapsulation efficiency was 56.62±2.43 %, cisplatin content was 389.47±13.88 mg/ml, quercetin encapsulation efficiency was calculated to be 62.01±1.22%, and quercetin content was 430.06±3.412 mg/ml.

### Fourier-transform infrared spectrum

Fig. 1 shows the FT-IR spectra of Eudragit® L-100, Qu (pure), physical mixture of Qu and Eudragit® L-100, and Qu-loaded NPs. Qu (pure) exhibited characteristic broad absorption bands at 3570.4 $cm^{-1}$ and 3246.6 $cm^{-1}$, which is consistent with phenolic O-H stretch vibrations. The aryl ketonic (C=O) stretch vibrations were observed at 1667.4 $cm^{-1}$. The absorption peaks at 1610.2 $cm^{-1}$, 1520.6 $cm^{-1}$, and 1452.5 $cm^{-1}$ were attributed to C-C, C=O, and C=C aromatic stretching vibrations, respectively. The OH bending vibrations of phenols occurred at 1377.2 $cm^{-1}$. The absorption peak at 1319.9 $cm^{-1}$, along with peaks between 950 $cm^{-1}$ and 600 $cm^{-1}$, were attributed to C-H bending vibrations of aromatic hydrocarbons. The C-O stretching vibrations of aryl ethers and phenols were found at 1262 $cm^{-1}$ and 1200 $cm^{-1}$, respectively. The observation of C-CO-C stretching and bending vibrations of ketones at 1169 $cm^{-1}$ supports the identification of the compound as the flavonoid Qu, in line with the findings of [23]. The FT-IR spectrum of Eudragit® L-100 polymer showed bands corresponding to O-H stretching (3400-3700 $cm^{-1}$). This band is typically broad and indicates the presence of hydroxyl groups (alcohols or phenols) in the polymer. The absorption band at 2800-3100 $cm^{-1}$ is associated with the stretching vibrations of the aliphatic C-H bonds in the polymer's backbone. The vibrations at 1600-1800 $cm^{-1}$ corresponds to the stretching vibration of the carbonyl group (C=O) in the polymer, which is likely from the methacrylic acid units. When Qu and Eudragit® L-100 were physically mixed, the resulting mixture showed absorption bands characteristic of both compounds. The respective frequencies at which these bands were detected were 3405 $cm^{-1}$, 3326.6 $cm^{-1}$, 1667 $cm^{-1}$, 1613.6 $cm^{-1}$, 1015.3 $cm^{-1}$, and 826.58 $cm^{-1}$. The most prominent absorption bands were observed at 3407.4 $cm^{-1}$, 2932.3 $cm^{-1}$, 2370.7 $cm^{-1}$, 1733.8 $cm^{-1}$, 1644.6 $cm^{-1}$, 1455.0 $cm^{-1}$, and 1059.4 $cm^{-1}$. The spectra of the Qu-loaded NPs showed the disappearance of the phenolic O-H stretch of Qu, and some peaks unique to the Qu-loaded NPs formulation were observed. In the Qu-loaded NPs formation, a decrease in the intensity and broadening of the O-H stretch peak, occurring between 3435 $cm^{-1}$ and 4144 $cm^{-1}$, was observed. This phenomenon could be attributed to the formation of intermolecular hydrogen bonding interactions between Qu and Eudragit® L-100. Studies have shown that hydrogen bonding can influence the transition from the crystalline state of Qu to the amorphous state [7, 24]. FTIR spectra were obtained from

pure cisplatin, Eudragit® L-100, the physical mixture of cisplatin and Eudragit®L-100, blank NPs, and cis loaded-NPs formulation. The cisplatin (pure) exhibited characteristic peaks, including those for amine stretching (3400–3200 cm$^{-1}$) [37], asymmetric amine bending (1625–1540 cm$^{-1}$), and symmetric amine bending (1300–1315 cm$^{-1}$) regions, as well as chloride stretching (796.58 cm$^{-1}$), [38] which is in agreement with a previous investigation [39]. The FTIR spectrum of the Eudragit® L-100 polymer demonstrated bands corresponding to O-H stretching (3400–3700 cm$^{-1}$), sp$^3$ C-H stretching (2800–3100 cm$^{-1}$), and C=O stretching (1600–1800 cm$^{-1}$). The physical mixture of cisplatin and Eudragit®L-100 exhibited absorption bands associated with both compounds at 3285.9, 3203.3, 1718.7, 1539.5, and 896.4 cm$^{-1}$. The FTIR spectrum after the encapsulation of cisplatin demonstrated two peaks at 2932.7 and 3387 cm$^{-1}$ (related to asymmetric and symmetric stretching of the-NH amine group, respectively) and 1640 and 1344 cm$^{-1}$ (related to the HNH asymmetric and symmetric bending, respectively). The

major absorption bands were observed at 3390.3, 2932.1, 2362.9, 2341.2, and 1734.0 cm$^{-1}$. These spectra revealed certain peaks that were unique to the cis-NP formulation and some that were associated with either the pure components or the physical mixture of the components and blank NPs. We also observed a broadening and decrease in the intensity of the O-H stretching peak (3000–3600 cm$^{-1}$). When Qu and Cis were mixed with Eudragit® L-100 together, the resulting compound showed characteristic absorption bands of (Qu-Cis) with the polymer compounds similar to pure Qu, Cis, and physical mixtures but at lower frequencies. The particular frequencies at which these bands were detected are as follows: 2332.5 cm$^{-1}$, 3750.3 cm$^{-1}$, and 2362.7 cm$^{-1}$; the FT-IR spectrum that represents the co-loaded (Qu-Cis)-NPs formulation observed a broadening and decrease in the intensity of the O-H stretching peak (3200-3600 cm$^{-1}$) due to the formation of intermolecular H-bonding interactions between (Qu-Cis) and Eudragit®L-100 during the formation of the NPs.
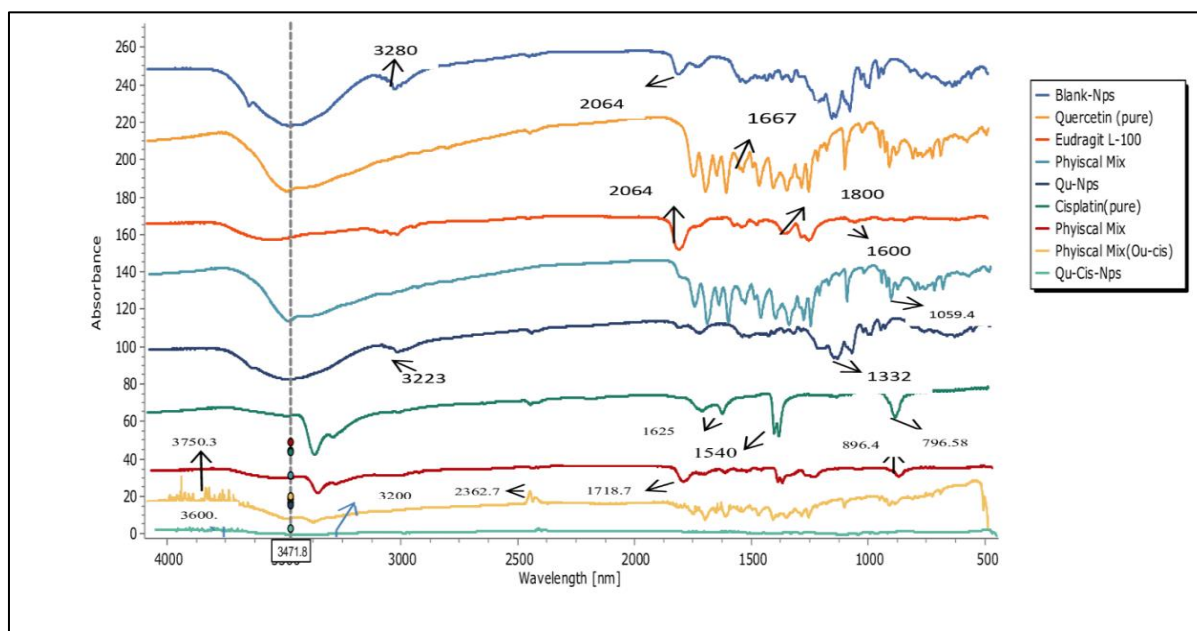


**Fig. 1: FT-IR spectra of blank NPs, Qu (pure), Eudragit® L-100, Physical mixture of (Qu/Eudragit® L-100), Qu-loaded NPs, Cis (pure), Physical mixture of (Cis/Eudragit® L-100), Cis-loaded NPs, Physical mixture (Qu-Cis/Eudragit® L-100), (Qu-Cis)-NPs**

**Powder X-ray diffraction**

X-ray diffraction analysis of Nanoparticles (NPs) provides valuable information about the shape, size, orientation, and molecular arrangement of ordered regions. Fig. 2 displays a comparison of the structural properties of blank NPs, Qu (pure), Eudragit® L-100, a physical mixture of Qu and Eudragit® L-100, and Qu-loaded NPs. The diffractogram of blank NPs showed multiple peaks at various angles, with the largest ones at 11.51°, 15.53°, 18.5°, 19.5°, 23.5°, and 28.5°. For pure Qu, five distinct, highly intense peaks were observed at 10.9°, 12.27°, 15.57°, 16.5°, and 27°, indicating its crystalline structure [34]. Eudragit® L-100 exhibited a single peak at 15°–20°, indicating a partial amorphous structure. When Qu and Eudragit® L-100 were physically combined, several spectral peaks of varying intensities were observed at 10.89°, 12.0°, 15.95°, 24.09°, and 27°. The weak peaks resembled those of Qu (pure), while the single, broad-profiled peak can be attributed to Eudragit® L-100. The reduced intensity of Qu peaks in the physical mixture was attributed to the lower amount of Qu and interference with Eudragit® L-100 molecule [25]. The nanoprecipitation technique was used to prepare Qu-loaded NPs, which produced a diffraction pattern indicating an amorphous state [26]. The DSC analysis confirmed that when Qu was loaded into the NPs, it transformed into an amorphous state. Despite having low-intensity peaks like the blank NPs, Qu-loaded NPs exhibited multiple peaks at 11.76°, 13.52°,

18.38°, 19.78°, 22.38°, and 24.38°, resulting in 81.8% crystallinity. This result can be attributed to the crystallization of Qu-loaded NPs, which occurs when Qu fills empty space in the NPs [27]. Similar observations have been reported by other researchers using other types of polymers [28, 29]. This could explain the increased crystallinity after entrapping the drug. Another possible explanation is that hydrophilic surfactants (stabilisers) dissolve in water rather than an organic solvent, giving the finished product a more crystalline appearance [30]. The nanoprecipitation techniques used to prepare the optimized Qu-loaded NPs allow the amorphous state to easily transition to the crystalline state [26].

which is a physical mixture of cisplatin and cis-loaded NPs. Five distinct, highly intense peaks appeared at 13.5°, 15°, 16.5°, 24°, and 26.5° due to the presence of Pt in the powder sample of pure cisplatin. The crystalline structure of cisplatin was responsible for these peaks. Moreover, the spectra exhibited a typical broad XRD peak of Eudragit L-100 from 10° to 25° in the diffraction pattern owing to its amorphous nature, indicating a partial amorphous structure of the mixture. To prepare optimized cis loaded-NPs, the amorphous state was changed into a crystalline state by using nanoprecipitation techniques [40]. In addition, because the hydrophilic surfactant was used in water instead of an organic solvent, the final product of NPs had a crystalline appearance [41]. The XRD peaks were observed at 13.5°, 15°, 16.5°, 24.09°, and

26.7° when cisplatin and Eudragit® L-100 were physically combined. The weak peaks were similar to those observed for pure cisplatin and Eudragit® L-100. The lower amount of cisplatin in the mixture, in addition to interference by the Eudragit® L-100 molecules, could be responsible for the reduced intensity of cisplatin peaks in the physical mixture. Many peaks at various angles were seen in the diffractogram of the blank NP, with the largest ones occurring at 11.51°, 15.53°, 18.5°, 19.5°, 23.5°, and 28.5°. The preparation of cis-loaded NPs via the nonparticipation technique resulted in a diffraction pattern similar to that of pure Eudragit® L-100. showing that cisplatin is transformed into an amorphous state after being loaded into NPs. The cis loaded-NPs exhibited multiple peaks at 11.56°, 12.11°, 15.56°, 18.59°, 19.48°,

and 24.38°. Despite having low-intensity peaks similar to those of blank NPs, cis loaded-NPs had 83.6% crystallinity. This can possibly be attributed to the crystallization of cis-loaded NPs, in which cisplatin fills the empty space in the NPs and contributes to improvement in the crystallinity [42]. This behavior may also explain the increased crystallinity of the cisplatin-loaded NPs after the drug was entrapped in the NPs. These results are in agreement with those obtained by previous studies. Finally, when Qu and Cis with Eudragit® L-100 were physically combined to prepare co-loaded (Qu-Cis)-NPs, several peaks of varying intensities were observed at 12°, 13.5°, 15°, 16.5°, and 24.09° degrees. The co-loaded (Qu-Cis)-NPs exhibited multiple peaks at 11.5°, 12.13°, 18.3°, 19.43°, and 24.38° degrees.
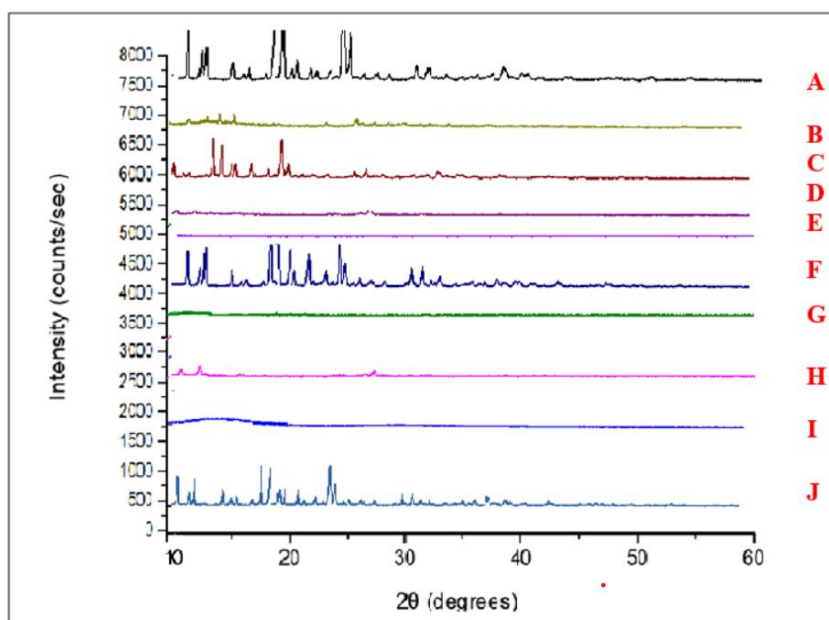


**Fig. 2: (A) Blank NPs, (B) Physical mixture (Qu-Cis/Eudragit® L-100), (C) Cis-loaded NPs, (D) physical mixture (Cis/Eudragit® L-100), (E) Cis (pure), (F) Qu-loaded NPs, G)Physical mixture (Qu/Eudragit® L-100, ), , , (H) Qu (pure), (I) Eudragit® L-100, (J), (Qu-Cis) NPs**
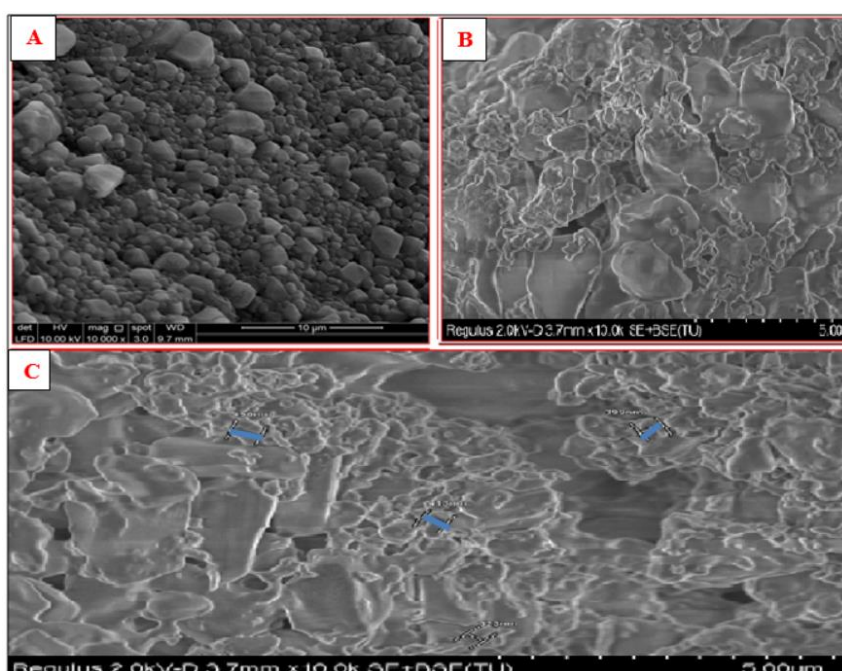


**Fig. 3: A. The scanning electron microscope images of blank NPs. Mag (10.000X), B, C. The ultra-electron microscope images of optimized co-loaded (Qu-Cis)-NPs (5.00 µm high-resolution scanning)**

**Cytotoxicity of co-loaded quercetin-cisplatin nanoparticle**

A cell viability study was conducted to assess the cytotoxic effect of co-loaded (Qu-Cis)-NPs on the non-small lung cancer cell line (NCI-H460) and normal human lung fibroblasts cell lines (CCD-19Lu) using the MTT assay. The cells were treated with different concentrations (0.031, 0.125, 0.063, 0.25, 0.5, and 1.0 mg/ml) of co-loaded (Qu-Cis)-NPs for 24 and 48 h of incubation. In fig. 4, 5, 6, and 7 show the viability of (NCI-H460) and (CCD-19Lu) cells, respectively, after 24 and 48 h of incubation. The results indicated that after 48 h of incubation, the co-loaded (Qu-Cis)-NPs exhibited greater cytotoxicity on the (NCI-H460) cancer cell line compared to Qu-loaded NPs and Cis-loaded NPs after 24 h of incubation, particularly at a concentration of 1 mg/ml. This optimal activity after 48 h is consistent with previous studies [43]. The cytotoxic effect depended on concentration-time-dependent effects. Higher concentrations of the drug are more effective due to a stronger dose-response relationship, leading to greater accumulation and cellular damage in cancer cells.

And sustained exposure to the drug allows for cumulative cytotoxicity, potentially leading to delayed but increased cell death over time. The co-loaded (Qu-Cis)-NPs produced a synergistic effect and higher cytotoxicity towards lung cancer cell lines [43]. This synergistic anticancer effect of both cis and Qu leads to enhanced therapeutic efficacy and complementary anticancer effects [44]. The cytotoxic effects of Qu are amplified when combined with cis [44]. As shown in fig. 8. According to these findings, the co-loaded (Qu-Cis)-NPs showed no cytotoxic effects on normal human lung fibroblasts cell lines (CCD-19Lu)cells at all concentrations (0.031, 0.063, 0.125, 0.25, 0.5, and 1.0 mg/ml) after 24 h of incubation. However, it exhibited cytotoxic effects on normal human lung fibroblasts cell lines (CCD-19Lu) cells, particularly at concentrations of 0.5 and 1.0 mg/ml, after 48 h of incubation. In clinical use**.** The absence of significant toxicity in normal cells supports the idea that this co-delivery system could be suitable for human trials, as it may provide therapeutic benefits without severe side effects.

**DISCUSSION**

The results demonstrate a significant synergistic effect of the co-delivery of quercetin and cisplatin in enhancing the therapeutic efficacy against lung cancer cells. This can be attributed to the complementary mechanisms of action of the two agents, where quercetin acts as an antioxidant and modulates signaling pathways, while cisplatin induces DNA damage and apoptosis. However, alternative explanations must be considered. One possibility is that the observed synergy could be due to improved cellular uptake and retention of both drugs when delivered together in nanoparticle form. The use of Eudragit L-100 may enhance the stability and targeted release of the drugs, allowing for a more localized and sustained effect, particularly in the tumor microenvironment. The findings are consistent with previous research that has demonstrated the potential of combination therapies in overcoming drug resistance and enhancing anti-cancer effects reported similar synergistic effects of quercetin and cisplatin in breast cancer cells, where quercetin sensitized the cells to cisplatin-induced apoptosis. However, our study differs in that we utilized Eudragit L-100 nanoparticles as the delivery system, which could explain the enhanced drug release in a pH-sensitive manner, leading to greater cytotoxic effects in lung cancer cells compared to free drug combinations in solution. Additionally, while other studies have focused on the role of quercetin in modulating oxidative stress and cisplatin's efficacy, our study uniquely examines the co-delivery system, emphasizing the benefits of nanoparticle encapsulation. One key difference in our results is the degree of enhancement in drug efficacy, which may be attributed to the increased stability and bioavailability of the drugs when delivered via Eudragit L-100.

One unexpected finding was the pronounced reduction in cell viability at lower concentrations of the drug combination, which contrasts with other reports where higher doses were required to observe significant cytotoxic effects. This could suggest that the nanoparticles not only enhance drug delivery but also improve drug retention within cancer cells, potentially due to the Eudragit L-100's pH sensitivity and its ability to release drugs more effectively in the

acidic tumor microenvironment. Another unexpected observation was that quercetin alone showed a relatively strong cytotoxic effect compared to its typical activity in other cancer cell types. This could be due to the specific characteristics of the lung cancer cell line used in this study, possibly indicating a heightened sensitivity to quercetin's effects on oxidative stress and apoptosis.

The results of this study reveal a significant synergistic effect of the co-delivery of quercetin and cisplatin in enhancing therapeutic efficacy against lung cancer cells. This synergy can be attributed to the complementary mechanisms of action where quercetin acts as an antioxidant and modulates signaling pathways, while cisplatin induces DNA damage and apoptosis. Similar synergistic effects have been reported in other studies. For instance, [45]. Demonstrated that quercetin enhanced the cytotoxicity of cisplatin in ovarian cancer cells through similar mechanisms, including modulation of oxidative stress and apoptotic pathways [45].

However, alternative explanations should be considered. One possibility is that the observed synergy could be due to improved cellular uptake and retention of both drugs when delivered in nanoparticle form. The use of Eudragit L-100 nanoparticles may enhance the stability and targeted release of the drugs, providing a more localized and sustained effect, particularly in the tumor microenvironment. This is consistent with the findings of [46], who reported that PLGA-based nanoparticles improved drug delivery and therapeutic outcomes by enhancing stability and controlling drug release [46]. Our study's use of Eudragit L-100 nanoparticles as the delivery system could explain the enhanced drug release in a pH-sensitive manner, leading to greater cytotoxic effects in lung cancer cells compared to free drug combinations in solution. This is in line with the work of [47], who observed that nanoparticles could significantly improve the efficacy of quercetin and other drugs through controlled release mechanisms [47].

A notable finding in our study was the pronounced reduction in cell viability at lower drug concentrations, contrasting with other reports where higher doses were required for significant cytotoxic effects. This suggests that the nanoparticles not only enhance drug delivery but also improve drug retention within cancer cells, potentially due to Eudragit L-100's pH sensitivity and its ability to release drugs more effectively in the acidic tumor microenvironment. This observation aligns with [48], who demonstrated that pH-sensitive nanoparticles could enhance drug release and efficacy in acidic environments [48]. Another unexpected finding was the relatively strong cytotoxic effect of quercetin alone, which differs from its typical activity in other cancer cell types. This heightened sensitivity could be attributed to the specific characteristics of the lung cancer cell line used in this study, indicating a potential increased responsiveness to quercetin's effects on oxidative stress and apoptosis. This is consistent with the findings of [49], who reported variable cytotoxic effects of quercetin in different cancer cell lines [49]. The potential mechanism of synergistic effects:-

1. Enhanced Cellular Uptake: Nanoparticles can improve cellular uptake through endocytosis, leading to higher intracellular concentrations of both quercetin and cisplatin. The pH-sensitive nature of Eudragit L-100 ensures that the drugs are released predominantly in acidic environments like the tumor, enhancing local drug delivery and reducing off-target effects. This mechanism has been well-documented, as noted by [44]. Apoptosis Pathways: Quercetin modulates multiple apoptosis pathways, including the inhibition of anti-apoptotic proteins such as Bcl-2 and the activation of pro-apoptotic proteins like Bax. This sensitizes cancer cells to cisplatin-induced apoptosis, as cisplatin primarily induces cell death through the mitochondrial pathway by causing DNA crosslinking and damage. These mechanisms were also highlighted in research by [50].

2. Overcoming Drug Resistance: Cisplatin resistance is often linked to increased DNA repair mechanisms and the upregulation of survival pathways like NF-KB. Quercetin is known to inhibit these pathways, potentially preventing the activation of survival mechanisms in response to cisplatin treatment. This aligns with the findings of [51], who investigated how quercetin could restore the efficacy of cisplatin in resistant cancer cells [51].
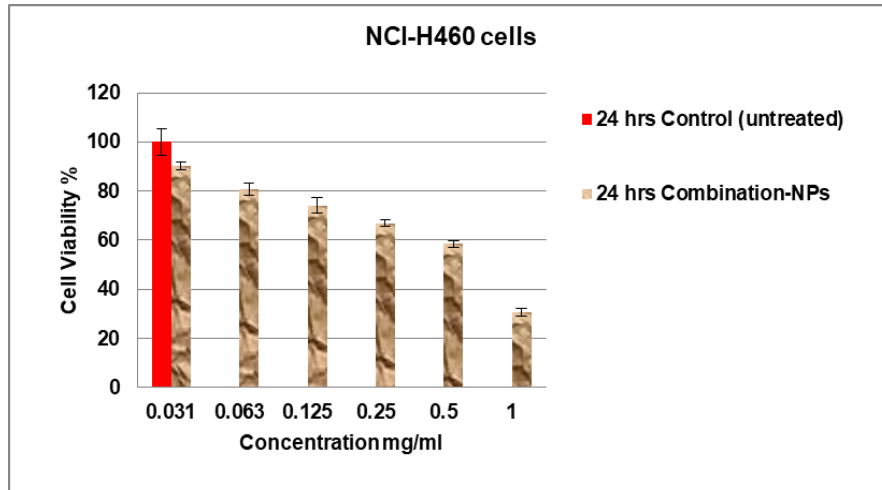
**Fig. 4: Cytotoxicity effects of (Qu-Cis)-NPs in NCI-H460 cells after 24 h of incubation. Data expressed as mean±SD, n=3**
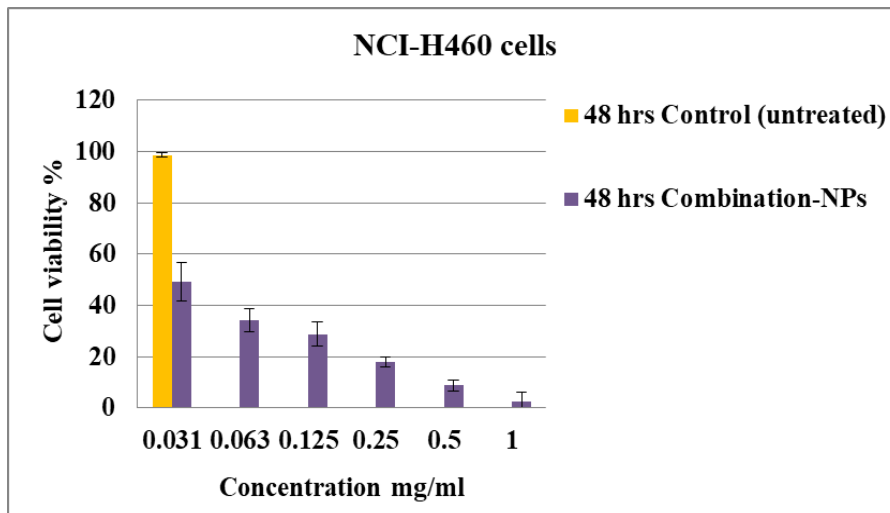


**Fig. 5: Cytotoxicity effects of (Qu-Cis)-NPs in NCI-H460 cells after 48 h of incubation. Data expressed as mean±SD, n=3**
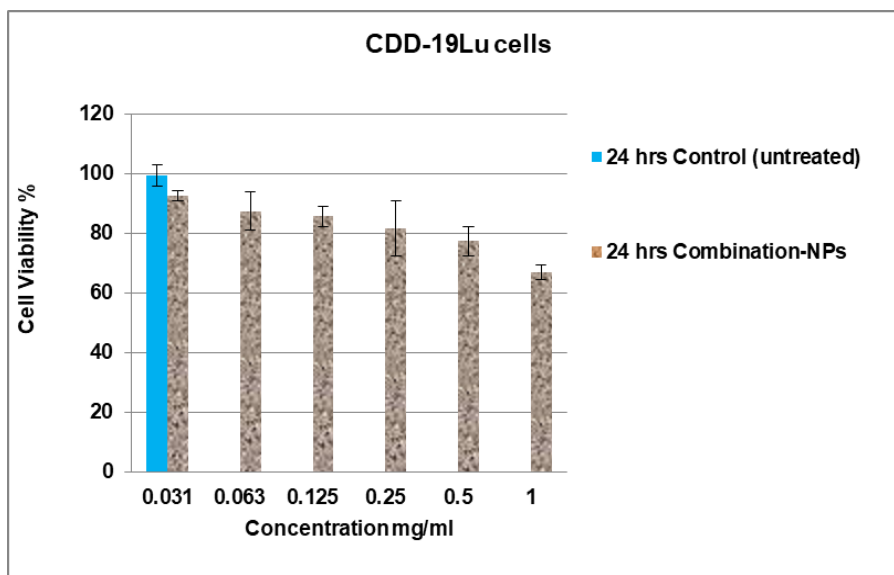


**Fig. 6: Cytotoxicity effects of (Qu-Cis)-NPs in CDD-19Lu cells after 24 h of incubation. Data expressed as mean±SD, n=3**
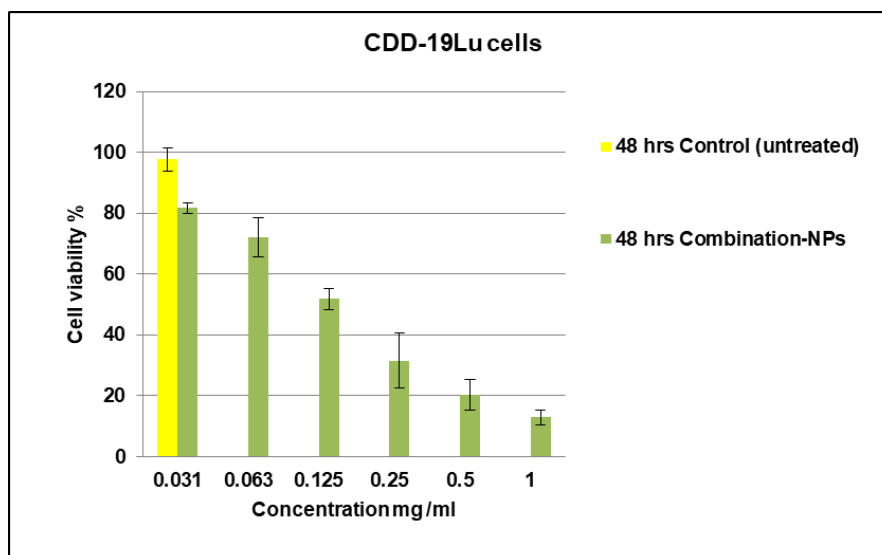
**Fig. 7: Cytotoxicity effects of (Qu-Cis)-NPs in CDD-19Lu cells after 48 h of incubation. Data expressed as mean±SD, n=3**
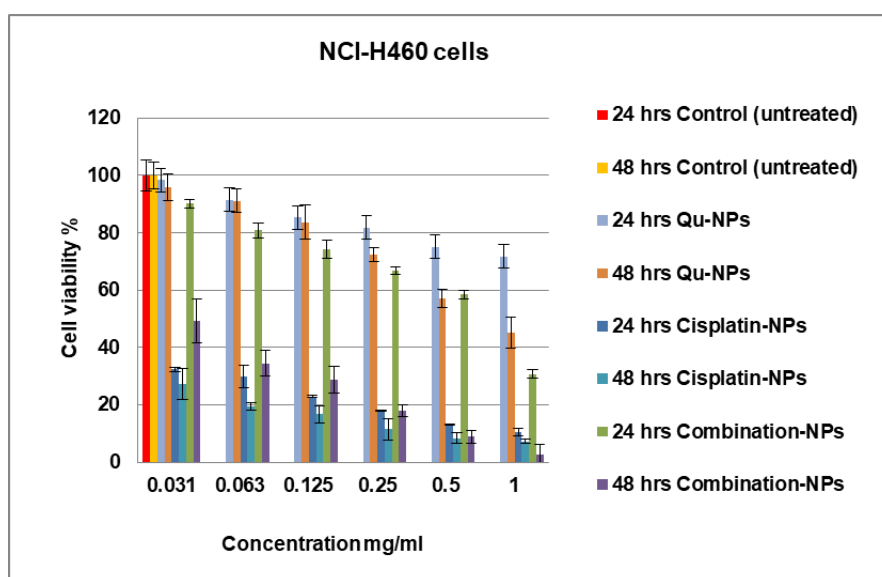


**Fig. 8: Cytotoxicity effects of (Qu-loaded NPs), (Cis-loaded NPs) and combination (Qu-Cis)-NPs in NCI-H460 cells after 24 and 48 h of incubation, data expressed as mean±SD, n=3**

## CONCLUSION

In this study, we present for the first time a nanoparticle formulation of co-loaded (Qu-Cis)NPs based on the pH-sensitive polymer Eudragit® L-100 for Lung-targeted delivery. Excellent drug entrapment efficiency and drug release profile were achieved with a nanoprecipitation-prepared formulation of Qu-loaded Eudragit®L-100 NPs. Intermolecular H-bonding between Qu and the polymer was detected by FT-IR and DSC studies, which demonstrated their compatibility. The NPs were found to contain Qu and Cis in an amorphous form, and the ionization of the carboxylate moieties in Eudragit®L100 NPs caused the medication to be released at neutral pH. (Qu-Cis)-loaded NPs showed a high and concentration-dependent toxicity to (NCI-H460) cancer cell line. These findings show that conventional pharmaceutical excipients such as Eudragit®L-100 can be used successfully in the production of nanomedicine. The successful development and Characterization of Eudragit® L-100 NPs open avenues for further research and optimisation, with potential implications for clinical translation. This research lays the foundation for future endeavours to refine and integrate this technology into clinical settings, ultimately contributing to advancements in cancer treatment strategies. This study not only adds to the growing body of knowledge in nanomedicine but also brings the field of medicine one step closer to realizing personalized and targeted therapies for cancer patients with few side effects, ultimately improving their quality of life. In conclusion, this study demonstrated that the co-delivery of quercetin and cisplatin via Eudragit L-100 nanoparticles offers a promising strategy for synergistic lung cancer therapy, exhibiting significant cytotoxicity against (NCI-H460) cancer cells while showing limited toxicity to normal lung cells. The concentration-and time-dependent effects observed highlight the therapeutic potential of this formulation. Moving forward, the next steps will involve conducting *in vivo* studies to assess the pharmacokinetics, biodistribution, and therapeutic efficacy of this nanoparticle system in animal models. These studies will provide critical insights into the formulation's safety and effectiveness in a physiological environment.

**AUTHORS CONTRIBUTIONS**

The authors hereby declare that the work presented in this article is original and that any liability for claims relating to the content of this article will be borne by them.

Firas F. Al-Mamoori: Contributed significantly to the conceptualization of the study, experimental design, data analysis, and interpretation. Was responsible for writing and revising the manuscript, and overseeing the overall research process.

Habibah A. Wahab: Supervised the research project, Assisted with the experimental design and implementation. Contributed to data collection analysis, and provided critical feedback on the manuscript.

Waqas Ahmad: Co-supervised the research project, provided guidance on experimental procedures, and contributed to the analysis and interpretation of data. Reviewed and edited the manuscript for intellectual content.

**CONFLICT OF INTERESTS**

The authors declare no conflict of interest.

**REFERENCES**

1. Services. Available from. https://www.who.int/news/item/01-02-2024-global-cancer-burden-growing--amidst-mounting-need-for-services.
2. The Lancet T. Globocan 2018: counting the toll of cancer. Lancet. 2018 Sep 22;392(10152):985. doi: 10.1016/S0140-6736(18)32252-9, PMID 30264708.
3. Siegel RL, Miller KD, Jemal A. Cancer statistics 2019. CA Cancer J Clin. 2019;69(1):7-34. doi: 10.3322/caac.21551, PMID 30620402.
4. World Health Organization (WHO). Cancer: 2020.
5. Zappa C, Mousa SA. Non-small cell lung cancer: current treatment and future advances. Transl Lung Cancer Res. 2016;5(3):288-300. doi: 10.21037/tlcr.2016.06.07, PMID 27413711.
6. WU Q, Yang Z, Nie Y, Shi Y, Fan D. Multidrug resistance in cancer chemotherapeutics: mechanisms and lab approaches. Cancer Lett. 2014;347(2):159-66. doi: 10.1016/j.canlet.2014.03.013, PMID 24657660.
7. Anwer MK, Al Mansoor MA, Jamil S, Al Shdefat R, Ansari MN, Shakeel F. Development and evaluation of PLGA polymer-based nanoparticles of quercetin. Int J Biol Macromol. 2016 Nov;92:213-9. doi: 10.1016/j.ijbiomac.2016.07.002, PMID 27381585.
8. Cetin M, Aktas Y, Vural I, Capan Y, Dogan LA, Duman M. Preparation and *in vitro* evaluation of bFGF loaded chitosan nanoparticles. Drug Deliv. 2007;14(8):525-9. doi: 10.1080/10717540701606483, PMID 18027182.
9. Adibkia K, Javadzadeh Y, Dastmalchi S, Mohammadi G, Niri FK, Alaei Beirami M. Naproxen eudragit RS100 nanoparticles: preparation and physicochemical characterization. Colloids Surf B Biointerfaces. 2011;83(1):155-9. doi: 10.1016/j.colsurfb.2010.11.014, PMID 21130612.
10. Russo M, Spagnuolo C, Tedesco I, Bilotto S, Russo GL. The flavonoid quercetin in disease prevention and therapy: facts and fancies. Biochem Pharmacol. 2012;83(1):6-15. doi: 10.1016/j.bcp.2011.08.010, PMID 21856292.
11. Cai X, Fang Z, Dou J, YU A, Zhai G. Bioavailability of quercetin: problems and promises. Curr Med Chem. 2013;20(20):2572-82. doi: 10.2174/09298673113209990120, PMID 23514412.
12. Mokale VJ, Naik JB, Verma U, Yadava SK. Preparation and characterization of biodegradable glimepiride loaded PLA nanoparticles by o/w solvent evaporation method using high-pressure homogenizer: a factorial design approach. SA J Pharm Pharmacol. 2018;1(1):1.
13. Adibkia K, Javadzadeh Y, Dastmalchi S, Mohammadi G, Niri FK, Alaei Beirami M. Naproxen eudragit RS100 nanoparticles: preparation and physicochemical characterization. Colloids Surf B Biointerfaces. 2011;83(1):155-9. doi: 10.1016/j.colsurfb.2010.11.014, PMID 21130612.
14. Song X, Zhao Y, Hou S, XU F, Zhao R, He J. Dual agents loaded PLGA nanoparticles: systematic study of particle size and drug entrapment efficiency. Eur J Pharm Biopharm. 2008;69(2):445-53. doi: 10.1016/j.ejpb.2008.01.013, PMID 18374554.
15. XU X, FU Y, HU H, Duan Y, Zhang Z. Quantitative determination of insulin entrapment efficiency in triblock copolymeric nanoparticles by high-performance liquid chromatography. J Pharm Biomed Anal. 2006;41(1):266-73. doi: 10.1016/j.jpba.2005.10.016, PMID 16303273.
16. Tantishaiyakul V, Phadoongsombut N, Kamaung S, Wongwisansri S, Mathurod P. Fourier transform infrared spectrometric determination of paracetamol and ibuprofen in tablets. Pharmazie. 2010;54(2):111-4.
17. Panwar P, Pandey B, Lakhera PC, Singh KP. Preparation characterization and *in vitro* release study of albendazole encapsulated nanosize liposomes. Int J Nanomedicine. 2010 Feb 25;5:101-8. doi: 10.2147/ijn.s8030, PMID 20309396.
18. Vaidya A, Jain A, Khare P, Agrawal RK, Jain SK. Metronidazole-loaded pectin microspheres for colon targeting. J Pharm Sci. 2009;98(11):4229-36. doi: 10.1002/jps.21742, PMID 19492406.
19. Van Meerloo J, Kaspers GJ, Cloos J. Cell sensitivity assays: the MTT assay. Methods Mol Biol. 2011;731:237-45. doi: 10.1007/978-1-61779-080-5_20.
20. Maeda H, Sawa T, Konno T. Mechanism of tumor-targeted delivery of macromolecular drugs including the EPR effect in solid tumor and clinical overview of the prototype polymeric drug SMANCS. J Control Release. 2001;74(1-3):47-61. doi: 10.1016/s0168-3659(01)00309-1, PMID 11489482.
21. Cho K, Wang X, Nie S, Chen ZG, Shin DM. Therapeutic nanoparticles for drug delivery in cancer. Clin Cancer Res. 2008;14(5):1310-6. doi: 10.1158/1078-0432.CCR-07-1441, PMID 18316549.
22. Wicki A, Witzigmann D, Balasubramanian V, Huwyler J. Nanomedicine in cancer therapy: challenges opportunities and clinical applications. J Control Release. 2015;200:138-57. doi: 10.1016/j.jconrel.2014.12.030, PMID 25545217.
23. Chourasiya A, Upadhaya A, Shukla RN. Isolation of quercetin from leaves of Azadirachta indica and antidiabetic study of the crude extracts. J Pharm Biomed Sci. 2018;25:179-81.
24. Abd El Rahman SN, Suhailah S. Quercetin nanoparticles: preparation and characterization. Indian J Drugs. 2016;2(3):96-103.
25. Mohammadi G, Mirzaeei S, Taghe S, Mohammadi P. Preparation and evaluation of eudragit® l100 nanoparticles loaded impregnated with KT tromethamine loaded PVA-HEC insertions for ophthalmic drug delivery. Adv Pharm Bull. 2019;9(4):593-600. doi: 10.15171/apb.2019.068, PMID 31857963.
26. Govender T, Stolnik S, Garnett MC, Illum L, Davis SS. PLGA nanoparticles prepared by nanoprecipitation: drug loading and release studies of a water-soluble drug. J Control Release. 1999;57(2):171-85. doi: 10.1016/s0168-3659(98)00116-3, PMID 9971898.
27. Verma A, Stellacci F. Effect of surface properties on nanoparticle cell interactions. Small. 2010;6(1):12-21. doi: 10.1002/smll.200901158, PMID 19844908.
28. Kakran M, Sahoo NG, Bao H, Pan Y, LI L. Functionalized graphene oxide as nanocarrier for loading and delivery of ellagic acid. Curr Med Chem. 2011;18(29):4503-12. doi: 10.2174/092986711797287548, PMID 21864287.
29. Zhang T, MA J, LI C, Lin K, Lou F, Jiang H. Core shell lipid polymer nanoparticles for combined chemo and gene therapy of childhood head and neck cancers. Oncol Rep. 2017;37(3):1653-61. doi: 10.3892/or.2017.5365, PMID 28098869.
30. Trenkenschuh E, Friess W. Freeze drying of nanoparticles: how to overcome colloidal instability by formulation and process optimization. Eur J Pharm Biopharm. 2021 Aug;165:345-60. doi: 10.1016/j.ejpb.2021.05.024, PMID 34052428.
31. Moustafine RI, Zaharov IM, Kemenova VA. Physicochemical characterization and drug release properties of eudragit E PO/eudragit L 100-55 interpolyelectrolyte complexes. Eur J Pharm Biopharm. 2006;63(1):26-36. doi: 10.1016/j.ejpb.2005.10.005, PMID 16380241.
32. Pecorini G, Ferraro E, Puppi D. Polymeric systems for the controlled release of flavonoids. Pharmaceutics. 2023;15(2):628. doi: 10.3390/pharmaceutics15020628, PMID 36839955.

33. Derakhshandeh K, Soheili M, Dadashzadeh S, Saghiri R. Preparation and *in vitro* characterization of 9-nitro camptothecin loaded long circulating nanoparticles for delivery in cancer patients. Int J Nanomedicine. 2010 Aug 9;5:463-71. doi: 10.2147/ijn.s11586, PMID 20957168.

34. Aldemir M, Okulu E, Kosemehmetoglu K, Ener K, Topal F, Evirgen O. Evaluation of the protective effect of quercetin against cisplatin-induced renal and testis tissue damage and sperm parameters in rats. Andrologia. 2014;46(10):1089-97. doi: 10.1111/and.12197, PMID 24266675.

35. Mokale VJ, Naik JB, Verma U, Yadava SK. Preparation and characterization of biodegradable glimepiride loaded PLA nanoparticles by o/w solvent evaporation method using high-pressure homogenizer: a factorial design approach. SAJ Pharm Pharmacol. 2019;1(1):1.

36. Chitkara D, Nikalaje SK, Mittal A, Chand M, Kumar N. Development of quercetin nanoformulation and *in vivo* evaluation using streptozotocin-induced diabetic rat model. Drug Deliv Transl Res. 2012 Apr;2(2):112-23. doi: 10.1007/s13346-012-0063-5.

37. Danhier F, Ansorena E, Silva JM, Coco R, LE Breton A, Preat V. PLGA based nanoparticles: an overview of biomedical applications. J Control Release. 2012;161(2):505-22. doi: 10.1016/j.jconrel.2012.01.043, PMID 22353619.

38. Wicki A, Witzigmann D, Balasubramanian V, Huwyler J. Nanomedicine in cancer therapy: challenges opportunities and clinical applications. J Control Release. 2015 Feb 28;200:138-57. doi: 10.1016/j.jconrel.2014.12.030, PMID 25545217.

39. Jain A, Jain SK. Engineered PLGA nanoparticles: an emerging therapeutic tool to treat lung cancer. Mol Pharm. 2013;10(3):838-45.

40. WU TH, Yen FL, Lin LT, Tsai TR, Lin CC, Cham TM. Preparation physicochemical characterization and antioxidant effects of quercetin nanoparticles. Int J Pharm. 2008;346(1-2):160-8. doi: 10.1016/j.ijpharm.2007.06.036, PMID 17689897.

41. Verma N, Tiwari A, Bajpai J, Bajpai AK. Swelling triggered release of cisplatin from gelatin-coated gold nanoparticles. Inorg Nano Met Chem. 2022;52(7):961-73. doi: 10.1080/24701556.2021.2025396.

42. Zhao H, Gagnon J, Hafeli UO. Process and formulation variables in the preparation of injectable and biodegradable magnetic microspheres. Biomagn Res Technol. 2007;5:2. doi: 10.1186/1477-044X-5-2, PMID 17407608.

43. Mori H, Niwa K, Zheng Q, Yamada Y, Sakata K, Yoshimi N. Cell proliferation in cancer prevention; effects of preventive agents on estrogen related endometrial carcinogenesis model and on an *in vitro* model in human colorectal cells. Mutat Res. 2001 Sep 1;(480-1):201-7. doi: 10.1016/s0027-5107(01)00200-7, PMID 11506814.

44. Zhang Y, Chan HF, Leong KW. Advanced materials and processing for drug delivery: the past and the future. Adv Drug Deliv Rev. 2013;65(1):104-20. doi: 10.1016/j.addr.2012.10.003, PMID 23088863.

45. Khan M, Khan M, Zhang H. Synergistic effect of quercetin and cisplatin in ovarian cancer cells: mechanistic insight into apoptosis and oxidative stress. Cancer Lett. 2019;452:270-80. doi: 10.1016/j.canlet.2019.01.038.

46. Danhier F, Ansorena E, Silva JM, Coco R, LE Breton A, Preat V. PLGA based nanoparticles: an overview of biomedical applications. J Control Release. 2012;161(2):505-22. doi: 10.1016/j.jconrel.2012.01.043, PMID 22353619.

47. WU TH, Yen FL, Lin LT, Tsai TR, Lin CC, Cham TM. Preparation physicochemical characterization and antioxidant effects of quercetin nanoparticles. Int J Pharm. 2008;346(1-2):160-8. doi: 10.1016/j.ijpharm.2007.06.036, PMID 17689897.

48. Zhao H, Gagnon J, Hafeli UO. Process and formulation variables in the preparation of injectable and biodegradable magnetic microspheres. Biomagn Res Technol. 2007;5:2. doi: 10.1186/1477-044X-5-2, PMID 17407608.

49. Verma N, Tiwari A, Bajpai J, Bajpai AK. Swelling triggered release of cisplatin from gelatin-coated gold nanoparticles. Inorg Nano Met Chem. 2022;52(7):961-73. doi: 10.1080/24701556.2021.2025396.

50. Mori H, Niwa K, Zheng Q, Yamada Y, Sakata K, Yoshimi N. Cell proliferation in cancer prevention; effects of preventive agents on estrogen related endometrial carcinogenesis model and on an *in vitro* model in human colorectal cells. Mutat Res. 2001;480-481:201-7. doi: 10.1016/s0027-5107(01)00200-7, PMID 11506814.

51. Zhang Y, Chan HF, Leong KW. Advanced materials and processing for drug delivery: the past and the future. Adv Drug Deliv Rev. 2013;65(1):104-20. doi: 10.1016/j.addr.2012.10.003, PMID 23088863.